inorganics

MDPI

Article

Tetramethylcyclopentadienyl Samarium(II) Metallocene Chemistry: Isolation of a Bimetallic Sm(II)/Sm(II) Complex

Joseph Q. Nguyen, Joseph W. Ziller and William J. Evans *

Department of Chemistry, University of California, Irvine, CA 92697-2025, USA
* Correspondence: wevans@uci.edu

Abstract: The salt metathesis reaction between one equivalent of $SmI_2(THF)_2$ and two equivalents of $K(C_5Me_4H)$ in THF afforded single crystals of the unusual, toluene-soluble, and asymmetric bimetallic Sm(II)/Sm(II) complex, $(C_5Me_4H)_2Sm^{II}(\mu\text{-}\eta^3\text{:}\eta^5\text{-}C_5Me_4H)Sm^{II}(C_5Me_4H)(THF)_2$, instead of the expected product, $(C_5Me_4H)_2Sm^{II}(THF)_2$. The toluene-insoluble products of this reaction can be worked up in 1,2-dimethoxyethane (DME) to provide X-ray quality crystals of the monomeric Sm(II) metallocene, $(C_5Me_4H)_2Sm^{II}(DME)$. $(C_5Me_4H)_2Sm^{II}(DME)$ can also be synthesized directly by the reaction between one equivalent of $SmI_2(THF)_2$ and two equivalents of $K(C_5Me_4H)$ in neat DME. The isolation and characterization of the bimetallic Sm(II)/Sm(II) complex provides supporting evidence for the possible oligomerization that may occur during the synthesis of Sm(II) complexes with cyclopentadienyl ligands that are less sterically bulky and less solubilizing than $(C_5Me_5)^{1-}$.

Keywords: samarium; tetramethylcyclopentadienyl; metallocene; bimetallic; bridging cyclopentadienyl; organometallic

check for updates

Citation: Nguyen, J.Q.; Ziller, J.W.; Evans, W.J. Tetramethylcyclopentadienyl Samarium(II) Metallocene Chemistry: Isolation of a Bimetallic Sm(II)/Sm(II) Complex. *Inorganics* **2023**, *11*, 4. https://doi.org/10.3390/inorganics11010004

Academic Editors: Leonor Maria and Joaquim Marçalo

Received: 1 December 2022
Revised: 16 December 2022
Accepted: 17 December 2022
Published: 21 December 2022

1. Introduction

The synthesis and isolation of the first soluble organometallic Sm(II) complexes, $(C_5Me_5)_2Sm(THF)_2$ [1] and $(C_5Me_5)_2Sm$ [2], in 1981 and 1984, respectively, propelled progress in organosamarium(II) chemistry by being suitable complexes for a series of reactivity studies that showcased the strong reducing properties of the Sm(II) ion in an organometallic environment. Some early representative examples included the reductive homologation of CO [3], the coupling of alkynes and alkenes with CO [4,5], the generation of unusual olefin dianions [6,7], and the first example of dinitrogen reduction by an *f*-element [8]. Subsequently, this system was explored broadly in many areas [9–25].

The pentamethylcyclopentadienyl ligand used in these studies was critical for providing the steric crowding required for isolating the monomeric Sm(II) complexes, the solubility of the Sm(II) complexes essential for reactivity, and the crystallinity of the paramagnetic Sm(III) products necessary for characterization using single-crystal X-ray crystallography. The first Sm(II) cyclopentadienyl complex, $[(C_5H_5)_2Sm(THF)]_n$ [26], was reported much earlier, in 1969, but since this unsubstituted cyclopentadienyl complex is insoluble in most solvents, even in THF, it did not provide access to unusual Sm(II) reactivity. It also did not form single crystals suitable for X-ray diffraction. Likewise, $[(C_5MeH_4)_2Sm(THF)]_n$ [27,28] displays similar behavior. Since then, Sm(II) complexes using various substituted cyclopentadienyl ligands have been reported, including $(C_5{}^tBu_3H_2)_2Sm$ [29], $(C_5{}^iPr_5)_2Sm$ [29], $[C_5(2,5\text{-}Ph_2)(3,4\text{-}p\text{-}tol_2)H]_2Sm(THF)$ [30], $(C_5Ph_4H)_2Sm(THF)$ [30], $(C_9H_7)_2Sm(THF)$ [31], $(C_{13}H_9)_2Sm(THF)_2$ [31], $(C_5Me_4{}^iPr)_2Sm(THF)$ [32], $[C_5(SiMe_3)_3H_2][C_5(SiMe_3)_2H_3]Sm(THF)$ [33], $[C_5Me_4(CH_2C_{10}H_7)]_2Sm(THF)_2$ [34], $[C_5Me_4(CH_2C_{10}H_7)]_2Sm$ [34], $[(4\text{-}n\text{Bu-}C_6H_4)_5C_5)]_2Sm$ [35], $[(4\text{-Et-}C_6H_4)_5C_5)]_2Sm$ [36], $[(4\text{-}{}^i\text{Pr-}C_6H_4)_5C_5)]_2Sm$ [36], $[(C_5Me_4)SiMe_2(CH_2CH{=}CH_2)]_2Sm$ [37], $(C_5{}^iPr_4H)_2Sm$ [29,38], $(C_5Ph_5)_2Sm$ [30,39], and $[C_5(CH_2Ph)_5]_2Sm$ [40]; see Scheme 1. One commonality between these Sm(II) complexes is the use of sterically bulky and solubilizing substituents on the cyclopentadienyl ligands [41].

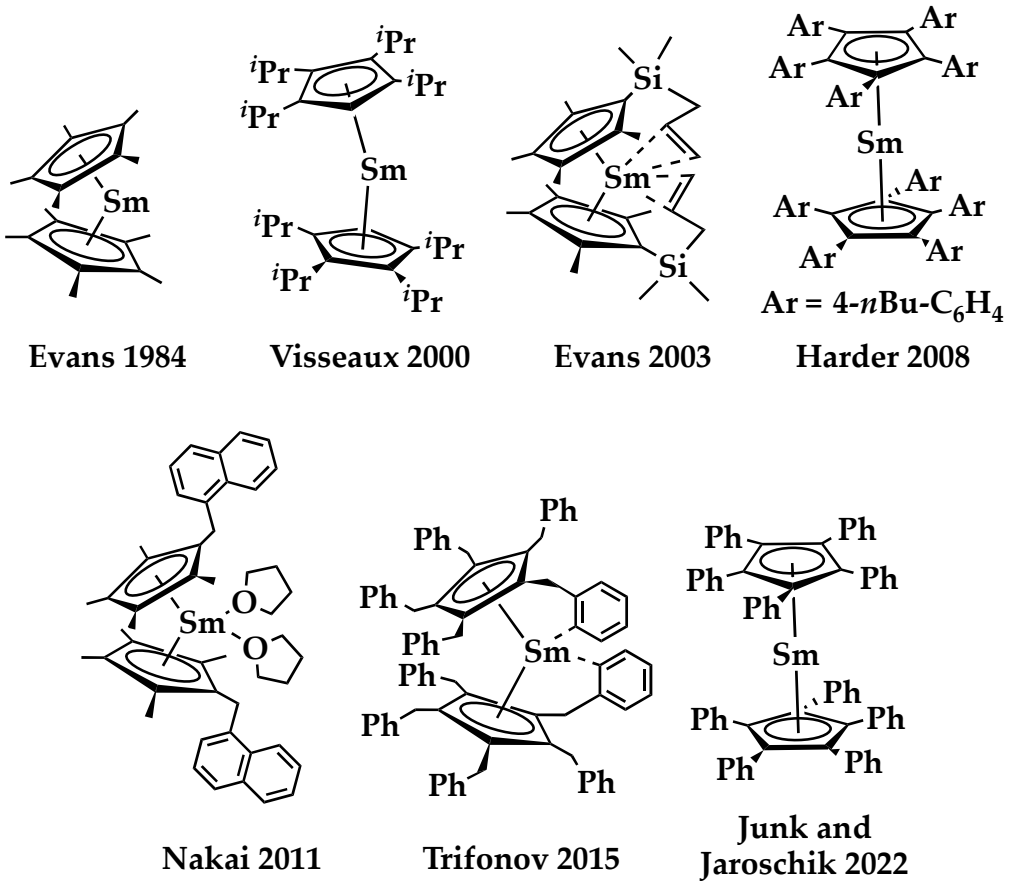

Scheme 1. Examples of crystallographically characterized Sm(II) metallocene complexes.

Although many of these Sm(II) metallocenes were characterizable by single-crystal X-ray crystallography, the tetramethylcyclopentadienyl Sm(II) complex, $(C_5Me_4H)_2Sm(THF)_2$ [42], closely related to $(C_5Me_5)_2Sm(THF)_2$, proved to be challenging to crystallize. Although spectroscopic data were reported for the product of the salt metathesis reaction between one equivalent of $SmI_2(THF)_2$ and two equivalents of $Na(C_5Me_4H)$, no crystallographic characterization of the isolated material was described, presumably due to the presence of complicating impurities [42]. Given that $(C_5Me_4H)_2Yb$ [43] and $(C_5Me_4H)_2Eu(THF)_2$ [44] were previously crystallographically characterized, we recently revisited the Sm(II) chemistry of this ligand as part of a broader study of $(C_5Me_4H)^{1-}$ *f*-element chemistry in our laboratory. Herein, we report two routes to crystallographically characterizable samarocenes involving this ligand.

2. Results

2.1. Synthesis and Structure of $(C_5Me_4H)_2Sm(DME)$, **2**

The reaction between two equivalents of $K(C_5Me_4H)$ and one equivalent of $SmI_2(THF)_2$ in THF at room temperature immediately produced a purple mixture and a white precipitate. Afterwards, centrifugation and filtration of the purple mixture to remove white insoluble solids, presumably KI, afforded a purple solution. Subsequently, purple solids were obtained from this purple solution upon removal of solvent from the supernatant under reduced pressure at room temperature. The vacuum was applied until the purple solids were dry enough to be a free-flowing powder. About 50–60% of the purple solids by mass were extracted with toluene to give a purple-green solution discussed later. However, about half of the purple solids remained undissolved despite multiple extractions in toluene, as shown in Scheme 2.

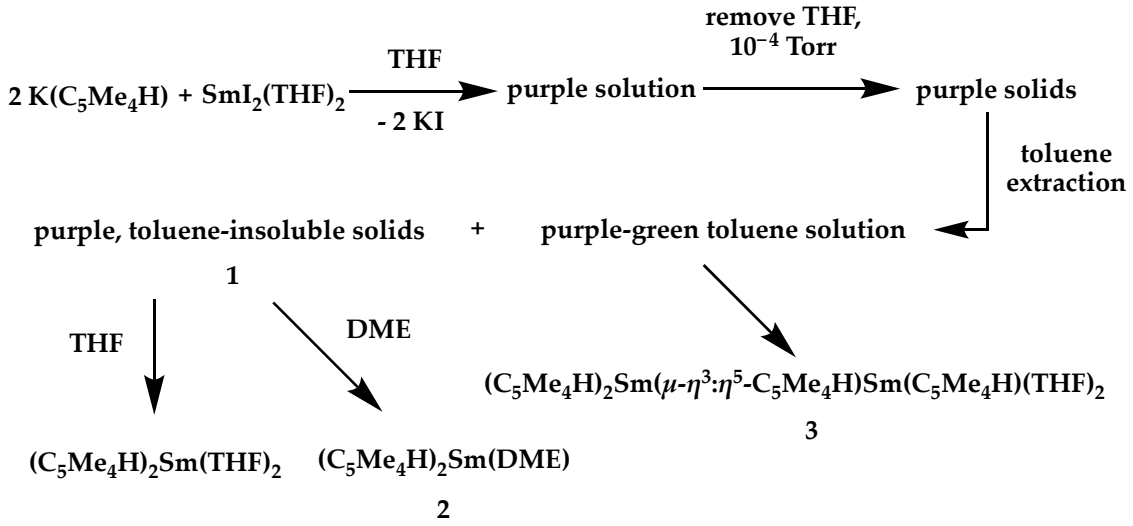

Scheme 2. Synthetic and workup procedure for the different products of the reaction between $SmI_2(THF)_2$ and 2 $K(C_5Me_4H)$ in THF.

The purple, toluene-insoluble solids, **1**, are also insoluble in alkanes, benzene, and diethyl ether. Elemental analysis suggested that compound **1** is $[(C_5Me_4H)_2Sm]_n$. However, incomplete combustion, which is commonly observed in organometallic *f*-element chemistry [45–49], was observed over multiple runs (see Experimental section). In support of this, **1** is soluble in THF and the ^1H NMR spectrum, taken in THF-d_8, matches the data reported for $(C_5Me_4H)_2Sm(THF)_2$ in 1995 [42], showing paramagnetically shifted resonances, which is typical for Sm(II) complexes; see Figure S1, Scheme 2 [1,2,29–40]. Despite multiple attempts, no X-ray quality crystals of this THF-solvated species could be grown in our hands which is consistent with the literature [42].

The addition of 1,2-dimethoxyethane (DME) to **1** at room temperature afforded a dark green solution which has a color similar to that of $(C_5Me_5)_2Sm(DME)$ [9]. Concentration of the dark green solution and overnight storage at −35 °C generated dark green crystals of $(C_5Me_4H)_2Sm(DME)$, **2**, which were suitable for study by X-ray diffraction, Figure 1, Scheme 2.

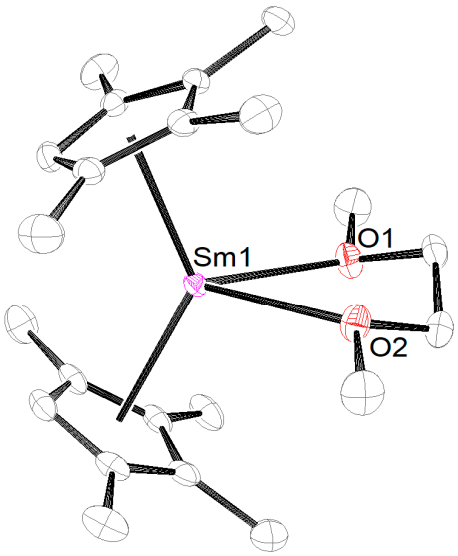

Figure 1. ORTEP representation of complex **2** with selective atom labeling. Ellipsoids are drawn at the 50% probability level. For clarity, hydrogen atoms and the second molecule in the asymmetric unit are not shown.

Complex **2** can also be synthesized directly by the reaction between K(C_5Me_4H) and $SmI_2(THF)_2$ in neat DME at room temperature, Scheme 3. The ^{1}H NMR spectrum of **2**, taken in THF-d_8, displays resonances corresponding to one type of $(C_5Me_4H)^{1-}$ environment as well as one molecule of DME per two $(C_5Me_4H)^{1-}$ ligands, Figure S2. Furthermore, the resonances are paramagnetically shifted, which is typical for a Sm(II) complex [1,2,29–40].

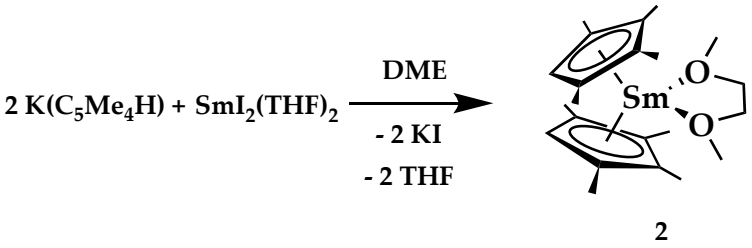

Scheme 3. Direct synthesis of $(C_5Me_4H)_2Sm(DME)$, **2**.

Complex **2** crystallizes in the orthorhombic *Pbca* space group with two crystallographically independent molecules in the asymmetric unit. Selected bond distances and angles for complex **2** are summarized in Table 1. Each molecule adopts a distorted tetrahedral geometry and is coordinated to two cyclopentadienyl ligands and the two oxygen atoms of a single DME molecule. The two molecules have similar metrical parameters; the Sm–C(C_5Me_4H) distances fall within the range of 2.741(2)–2.867(2) Å and the Cnt–Sm–Cnt (Cnt = ring centroid) angles are 130.3° for both molecules. Furthermore, the 2.591(1)–2.617(1) Å Sm–O(DME) distances is similar to the Sm–O(DME) distances in $(C_5Me_5)_2Sm(DME)$ [9]. However, the average O(DME)–Sm–O(DME) angle in complex **2** is 63.57(4)°, which is narrower than the 67.2(9)° seen in $(C_5Me_5)_2Sm(DME)$.

Table 1. Selected bond distances (Å) and angles (°) for $(C_5Me_4H)_2Sm(DME)$, **2**.

Sm(1)–O(1)	2.591(1)	Sm(2)–O(3)	2.612(1)
Sm(1)–O(2)	2.617(1)	Sm(2)–O(4)	2.601(1)
Sm(1)–C(1)	2.813(2)	Sm(2)–C(23)	2.794(2)
Sm(1)–C(2)	2.821(2)	Sm(2)–C(24)	2.830(2)
Sm(1)–C(3)	2.807(2)	Sm(2)–C(25)	2.824(2)
Sm(1)–C(4)	2.796(2)	Sm(2)–C(26)	2.786(2)
Sm(1)–C(5)	2.787(2)	Sm(2)–C(27)	2.760(2)
Sm(1)–C(10)	2.747(2)	Sm(1)–C(32)	2.810(2)
Sm(1)–C(11)	2.821(2)	Sm(1)–C(33)	2.826(2)
Sm(1)–C(12)	2.867(2)	Sm(1)–C(34)	2.834(2)
Sm(1)–C(13)	2.819(2)	Sm(1)–C(35)	2.819(2)
Sm(1)–C(14)	2.741(2)	Sm(1)–C(36)	2.787(2)
Sm(1)–Cnt(1)	2.534	Sm(2)–Cnt(3)	2.528
Sm(1)–Cnt(2)	2.527	Sm(2)–Cnt(4)	2.544
O(1)–Sm(1)–O(2)	63.92(4)	O(3)–Sm(2)–O(4)	63.21(4)
Cnt(1)–Sm(1)–Cnt(2)	130.3	Cnt(3)–Sm(2)–Cnt(4)	130.3

In each molecule of **2**, the hydrogen substituted carbon atoms on the cyclopentadienyl rings are at the back of the wedge where the two rings are closest to each other and have the most steric repulsion. The orientation of the $(C_5Me_4H)^{1-}$ rings with respect to each other is slightly different in the two molecules, Figure 2. One molecule has a H(C_5Me_4H) . . . H(C_5Me_4H) distance of 3.196 Å while the other molecule has an analogous distance of

3.683 Å. The fact that two different orientations with similar metrical parameters form the low energy structure that crystallizes suggests that there is no single preferred orientation. In contrast, $(C_5Me_5)_2Sm(DME)$ crystallizes as a single molecule in the asymmetric unit along with one molecule of DME in the lattice [9].

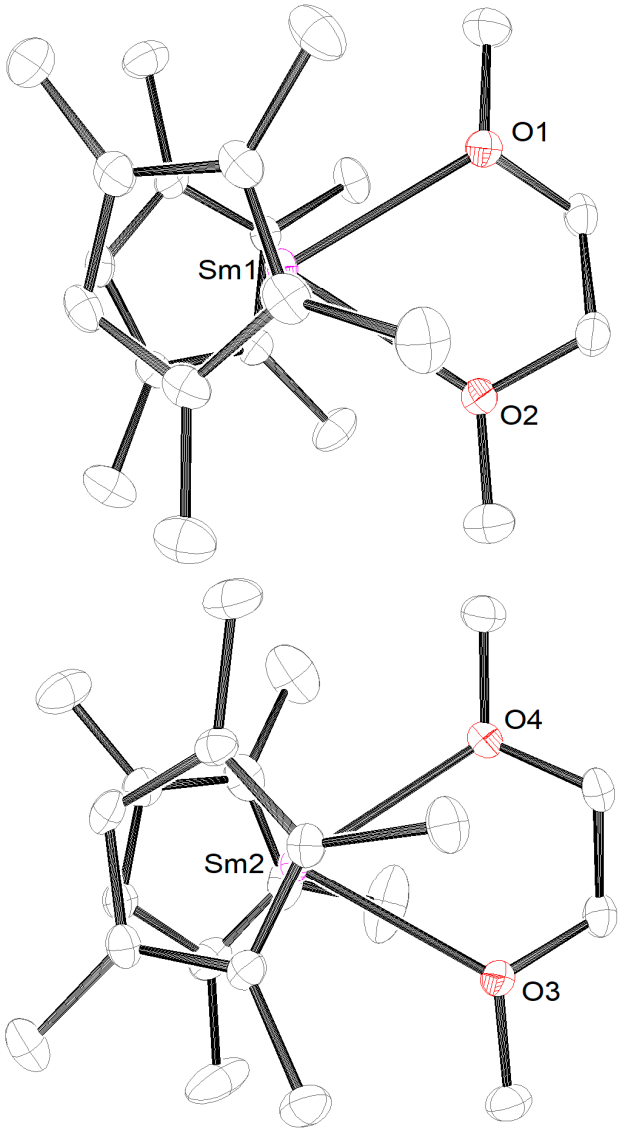

Figure 2. Top-down view of both molecules of $(C_5Me_4H)_2Sm(DME)$, **2,** in the asymmetric unit. For clarity, hydrogen atoms are not shown.

The metrical parameters of **2** are compared to those of other structurally characterized Sm(II) metallocenes in Table 2 and are ordered in increasing Cnt–Sm–Cnt angle. The Sm–Cnt distances in **2** fall within the range typically observed for a Sm(II) metallocene and not for a Sm(III) metallocene [1,2,31–40]. The Cnt–Sm–Cnt angle of **2** is the second smallest observed for a Sm(II) metallocene, behind the 126.4° seen in $(C_{13}H_9)_2Sm(THF)_2$ [31]. However, the more acute angle seen in $(C_{13}H_9)_2Sm(THF)_2$ is likely a consequence of $(C_{13}H_9)_2Sm(THF)_2$ having a noticeably longer Sm–Cnt distance than the other Sm(II) metallocenes in the literature.

Table 2. Comparison of Sm–Cnt (Å) and Sm–O (Å) distances and Cnt–Sm–Cnt angles (°) for various crystallographically characterized Sm(II) metallocenes in order of increasing Cnt–Sm–Cnt angle.

Complex	Sm–Cnt (Å)	Sm–O (Å)	Cnt–Sm–Cnt (°)
$(C_5Me_4H)_2Sm(\mu\text{-}\eta^3{:}\eta^5\text{-}C_5Me_4H)Sm(C_5Me_4H)(THF)_2$, **3** [a]	2.584, 2.581, 2.537, 2.586	2.577(2), 2.597(2)	122.8, 130.2
$(C_{13}H_9)_2Sm(THF)_2$ [31]	2.633, 2.629	2.560(6), 2.540(6)	126.4
$(C_5Me_4H)_2Sm(DME)$, **2** [a]	2.534, 2.527, 2.528, 2.544	2.591(1), 2.617(1), 2.601(1), 2.612(1)	130.3
$(C_5Me_5)_2Sm(THF)_2$ [1]	2.60	2.63(1)	136.7
$[C_5H_2(SiMe_3)_3][C_5H_3(SiMe_3)_2]Sm(THF)$ [33]	2.559, 2.553	2.547(3)	137.0
$[C_5Me_4(CH_2C_{10}H_7)]_2Sm$ [34]	2.533, 2.529	—	138.05(6)
$(C_5Me_5)_2Sm(THF)$ [33]	2.542, 2.549	2.569(3)	138.5
$[C_5Me_4(CH_2C_{10}H_7)]_2Sm(THF)_2$ [34]	2.576, 2.582	2.646(2), 2.590(2)	138.97(3)
$(C_5Me_5)_2Sm(DME)$ [9]	2.54, 2.57	2.52(1), 2.61(2)	140
$(C_5Me_5)_2Sm$ [2]	2.53	—	140.1
$[(C_5Me_4)SiMe_2(CH_2CH{=}CH_2)]_2Sm$ [37]	2.551	—	141.2
$(C_5Me_4{}^iPr)_2Sm(THF)$ [32]	2.531	2.540(5)	141.6
$[C_5(CH_2Ph)_5]_2Sm$ [40]	2.555, 2.565	—	141.8
$(C_5{}^iPr_4H)_2Sm$ [29,38]	2.51	—	152.0
$[(4\text{-}Et\text{-}C_6H_4)_5C_5)]_2Sm$ [36]	2.504, 2.521	—	166.9(1), 168.0(1)

[a] This work.

2.2. Synthesis and Structure of $(C_5Me_4H)_2Sm^{II}(\mu\text{-}\eta^3{:}\eta^5\text{-}C_5Me_4H)Sm^{II}(C_5Me_4H)(THF)_2$, **3**

The purple-green toluene solution obtained by extraction of the $SmI_2(THF)_2/K(C_5Me_4H)$ reaction mixture as described above led to the isolation of a different Sm(II) metallocene than **1** or **2**. Concentration and subsequent storage of the solution at −35 °C in the presence of THF generated purple, X-ray-quality crystals of the bimetallic complex, $(C_5Me_4H)_2Sm(\mu\text{-}\eta^3{:}\eta^5\text{-}C_5Me_4H)Sm(C_5Me_4H)(THF)_2$, **3**; see Figure 3, Scheme 2. Complete removal of the solvent resulted in the formation of green solids. However, these green solids exhibit low solubility in non-coordinating solvents, and no X-ray-quality single crystals have been isolated.

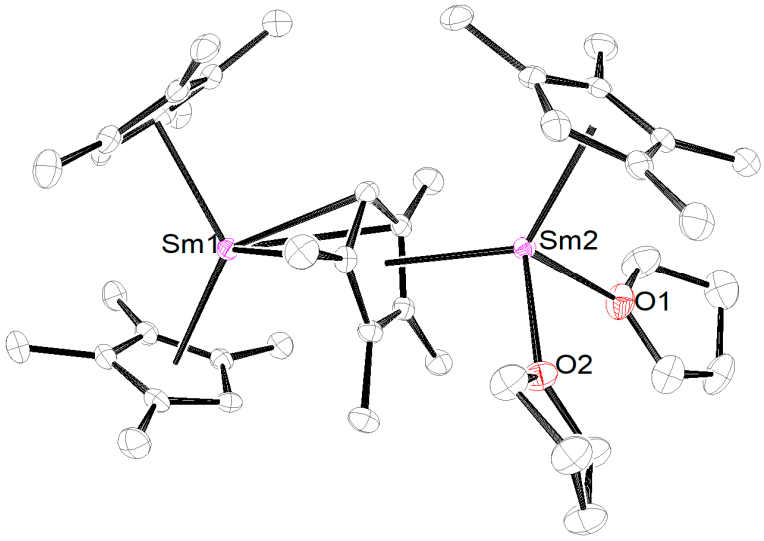

Figure 3. ORTEP representation of complex **3** with selective atom labeling. Ellipsoids are drawn at the 50% probability level. For clarity, hydrogen atoms are not shown.

Complex **3** crystallizes in the monoclinic $P2_1/n$ space group with a single molecule in the asymmetric unit. Complex **3** is an asymmetric, bimetallic Sm(II)/Sm(II) complex that consists of a desolvated [(η^5-$C_5Me_4H)_2$Sm] metallocene moiety and a disolvated [(μ-η^3:η^5-C_5Me_4H)(η^5-C_5Me_4H)Sm$(THF)_2$] metallocene moiety bridged by a $(C_5Me_4H)^{1-}$ ligand. A cyclopentadienyl-bridged bimetallic samarium complex has been observed previously in the literature. However, it is the mixed-valent Sm(II)/Sm(III) complex, $(C_5Me_5)_2Sm^{II}$(μ-η^5:η^5-C_5H_5)$Sm^{III}(C_5Me_5)_2$ [50], which contains five cyclopentadienyl rings instead of the four in complex **3**. Selected metrical parameters for complex **3** are summarized in Table 3 and are compared with other Sm(II) metallocenes in Table 2.

Table 3. Selected bond distances (Å) and angles (°) for ($C_5Me_4H)_2$Sm(μ-η^3:η^5-C_5Me_4H)Sm (C_5Me_4H)$(THF)_2$, **3**.

Sm(1)–C(1)	2.819(2)	Sm(2)–C(19)	2.814(2)
Sm(1)–C(2)	2.931(2)	Sm(2)–C(20)	2.806(2)
Sm(1)–C(3)	2.932(2)	Sm(2)–C(21)	2.804(2)
Sm(1)–C(4)	2.810(2)	Sm(2)–C(22)	2.811(2)
Sm(1)–C(5)	2.751(2)	Sm(2)–C(23)	2.799(2)
Sm(1)–C(10)	2.831(2)	Sm(2)–C(28)	2.835(2)
Sm(1)–C(11)	2.940(2)	Sm(2)–C(29)	2.872(2)
Sm(1)–C(12)	2.919(2)	Sm(2)–C(30)	2.888(2)
Sm(1)–C(13)	2.791(2)	Sm(2)–C(31)	2.864(2)
Sm(1)–C(14)	2.748(2)	Sm(2)–C(32)	2.807(2)
Sm(1)–C(28)	2.962(2)	Sm(1)–C(31)	2.955(2)
Sm(1)–C(29)	3.160(2)	Sm(1)–C(32)	2.842(2)
Sm(1)–C(30)	3.153(2)	Sm(2)–Cnt(3)	2.537
Sm(1)–Cnt(1)	2.584	Sm(2)–Cnt(4)	2.586
Sm(1)–Cnt(2)	2.581	Cnt(3)–Sm(2)–Cnt(4)	130.2
Cnt(1)–Sm(1)–Cnt(2)	122.8	Sm(2)–O(1)	2.577(2)
Sm(2)–O(2)	2.597(2)		

The coordination sphere of Sm(2) in complex **3** with two (η^5-$C_5Me_4H)^{1-}$ rings and two THF molecules is most similar to that of complex **2** and $(C_5Me_5)_2Sm(THF)_2$ [1]. The 130.2° Cnt–Sm(2)–Cnt angle in **3** is equivalent to those in **2** and the 2.537 Å and 2.586 Å Sm(2)–Cnt distances are within a range typical for a Sm(II) metallocene [1,2,31–40]. Moreover, the Sm(2)–O(THF) distances of 2.577(2) Å and 2.597(2) Å are similar to the Sm–O(THF) distances of other crystallographically characterized Sm(II) metallocenes, as shown in Table 2.

Sm(1) has two (η^5-$C_5Me_4H)^{1-}$ ligands that have Sm(1)–C(C_5Me_4H) distances ranging from 2.748(2) Å to 2.940(2) Å. The 122.8° Cnt–Sm(1)–Cnt angle for the two (η^5-$C_5Me_4H)^{1-}$ ligands is much more bent than that of complex **2** because Sm(1) also has an (η^3-$C_5Me_4H)^{1-}$ ligand in its coordination sphere. In a sense, the Sm(1) moiety may be considered a Sm(II) analog with $(C_5Me_4H)^{1-}$ ligands of the Sm(III) complex, $(C_5Me_5)_2Sm(\eta^3$-$CH_2CHCH_2)$ [51]. However, the Sm(III) metallocene allyl complex has a Cnt–Sm–Cnt angle of 140.3°, presumably because it has Sm–C bond distances that are much shorter due to the metal center having a higher oxidation state than Sm(1) in complex **3**. The average Sm(1)–C(η^5-C_5Me_4H) distance in **3** is 2.847(2) Å, which is longer than the 2.724(30) Å average bond distance observed in $(C_5Me_5)_2Sm(\eta^3$-$CH_2CHCH_2)$. Similarly, the 2.842(2)–2.962(2) Å Sm(1)–C(η^3-C_5Me_4H) distances in **3** for the three closest ring carbon atoms are much longer than the 2.630(15)–2.668(18) Å Sm–C(CH_2CHCH_2) distances in $(C_5Me_5)_2Sm(\eta^3$-$CH_2CHCH_2)$.

This is consistent with the 0.1–0.2 Å differences typically observed between Sm(II)–C and Sm(III)–C distances in complexes featuring cyclopentadienyl or allyl ligands [1–8,51]. The other Sm(1)–C(η^3-C_5Me_4H) bond lengths in **3** for the two more distant carbon atoms in the cyclopentadienyl ligand are noticeably longer and are 3.153 Å and 3.160 Å.

The relatively small 122.8° Cnt–Sm(1)–Cnt angle in **3** is reminiscent of the 120° Cnt–Ln–Cnt angle observed in the sterically crowded $(C_5Me_5)_3Ln$ complexes that undergo sterically induced reduction [52]. One characteristic of $(C_5Me_5)_3Ln$ complexes that effect sterically induced reduction reactions is that they have at least one methyl substituent that is displaced from the average plane generated by the cyclopentadienyl ring by at least 0.48 Å [52]. However, the methyl displacements shown for complex **3** in Table 4 do not exceed 0.195 Å, and hence it cannot be considered sterically crowded by this criterion even though the Cnt–Sm–Cnt angle is very small [52].

Table 4. Displacements for the methyl substituents from the average ring carbon plane generated by the $(C_5Me_4H)^{1-}$ ligand (Å) and the (average ring carbon plane)–C(ring)–C(Me) angles (°) for Sm(1) in **3**.

Cnt(1) . . . C(6)	0.032 Å	0.67°	Cnt(2) . . . C(15)	0.041 Å	0.86°
Cnt(1) . . . C(7)	0.153 Å	3.25°	Cnt(2) . . . C(16)	0.146 Å	3.11°
Cnt(1) . . . C(8)	0.195 Å	4.15°	Cnt(2) . . . C(17)	0.144 Å	3.04°
Cnt(1) . . . C(9)	0.044 Å	0.93°	Cnt(2) . . . C(18)	0.055 Å	1.16°

The ^{1}H NMR spectrum of **3** in C_6D_6 has resonances that can be attributed to more than one type of $(C_5Me_4H)^{1-}$ ligand, but the paramagnetism of the Sm(II) complex precluded a definitive assignment; see Figure S3.

2.3. Infrared Spectroscopy and UV-Visible Spectroscopy

Infrared spectroscopy was used to characterize the purple, toluene-insoluble solids, **1**, obtained from the reaction between $SmI_2(THF)_2$ and $K(C_5Me_4H)$ in THF, and to compare to the infrared spectra of **2** and **3**; see Figure 4 and Figures S4–S6.

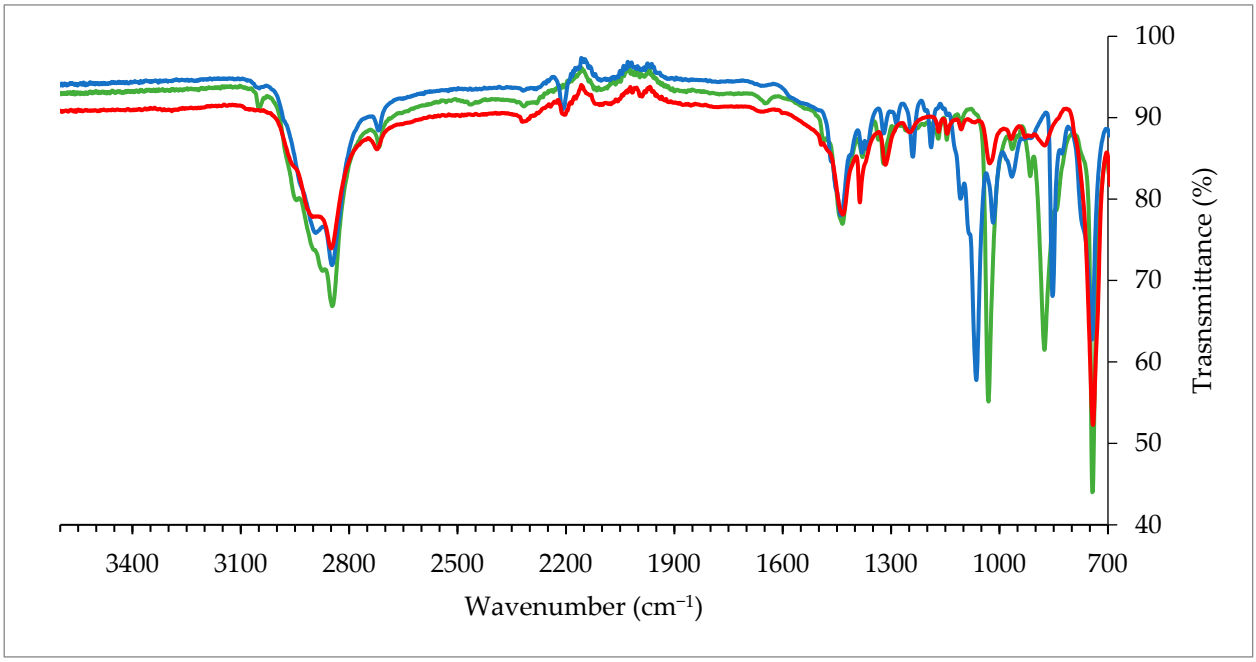

Figure 4. Infrared spectra of **1** (red), **2** (blue), and **3** (green).

The infrared spectra of **1, 2,** and **3** all display absorptions centered around 3000 cm^{-1} and 740 cm^{-1}, which is typical for the C–H stretching vibrations and bending vibrations of the cyclopentadienyl ligands [53], respectively. Another band centered around 1440 cm^{-1} is observed and is characteristic of C–C vibrations [53]. In addition, the infrared spectrum of **2** has two very strong bands at 1060 cm^{-1} and 860 cm^{-1}, diagnostic of coordination of an O-donor ligand on a metal center [54–56], which for complex **2** is DME. This compares well with the reported infrared data for $(C_5Me_5)_2Sm(DME)$, which also has the strong bands associated with coordination of a DME molecule at 1040 cm^{-1} and 860 cm^{-1} [9]. The infrared spectrum of **1** looks very similar to the infrared spectrum of **2**, except the bands at 1060 cm^{-1} and 860 cm^{-1} are not present; see Figure 4. This suggests that these purple, toluene-insoluble solids, **1**, are fully desolvated. This notion is further supported by the infrared spectrum of **3**, which has a similar spectrum to **2**, including the two very strong bands at 1030 cm^{-1} and 876 cm^{-1} corresponding to the THF molecules bound to **3**. These bands are similar to the ones found at 1040 cm^{-1} and 895 cm^{-1} in the infrared spectrum of $(C_5Me_5)_2Sm(THF)_2$, which are absent in $(C_5Me_5)_2Sm$ [1,2].

The UV-visible spectra of complex **1**, **2**, and **3** were also collected in THF at room temperature and were compared with the UV-visible spectrum of $(C_5Me_5)_2Sm(THF)_2$, as shown in Figures S7–S11. Despite the differences spectroscopically and structurally between **1**, **2**, and **3**, the UV-visible spectra are identical in THF and display absorptions centered around 390 nm and 550 nm. In comparison to $(C_5Me_5)_2Sm(THF)_2$, there are no noticeable differences. Additionally, no differences are observed whether the UV-visible spectrum of **3** is taken in THF or toluene.

3. Discussion

The reaction between $SmI_2(THF)_2$ and $K(C_5Me_4H)$ in DME readily forms single crystals of $(C_5Me_4H)_2Sm(DME)$, **2**, amenable to single-crystal X-ray crystallography. This contrasts with the same reaction in THF, where X-ray-quality crystals of the expected product, $(C_5Me_4H)_2Sm(THF)_2$, have proven elusive. This emphasizes the subtleties that are present in *f*-element organometallic chemistry. Further evidence on this point comes from the isolation of $(C_5Me_4H)_2Sm(\mu\text{-}\eta^3{:}\eta^5\text{-}C_5Me_4H)Sm(C_5Me_4H)(THF)_2$, **3**. The isolation of this asymmetric bimetallic complex that is composed of monometallic $[(C_5Me_4H)_2Sm]$ and $[(C_5Me_4H)_2Sm(THF)_2]$ moieties is most surprising.

On the basis of the structures of **2** and **3** and the spectroscopic data obtained in this study, it is likely that removal of solvent under reduced pressure from reactions between $SmI_2(THF)_2$ and $K(C_5Me_4H)$ generates an insoluble $[(C_5Me_4H)_2Sm]_n$ species that involves bridging $(C_5Me_4H)^{1-}$ ligands of the type found in **3**. If small amounts of THF are present, toluene-soluble compounds such as the bimetallic complex **3** can be isolated. In the presence of an excess of coordinating solvents such as THF or DME, $(C_5Me_4H)_2Sm(THF)_2$ and $(C_5Me_4H)_2Sm(DME)$ are likely to exist as monomeric species in solution.

These results with the $(C_5Me_4H)^{1-}$ ligand differ significantly from those of the $(C_5Me_5)^{1-}$ ligand. In the pentamethylcyclopentadienyl case, the unsolvated $(C_5Me_5)_2Sm$ can be isolated and crystallographically characterized. Evidently, the absence of one methyl group on the cyclopentadienyl ring allows bridging structures such as in **3** which may not be as energetically accessible as for $(C_5Me_5)_2Sm$. The fact that Sm(1) in **3** can achieve a Cnt–Sm–Cnt angle of 122.8°, the smallest observed for a Sm(II) metallocene, is consistent with this.

The structural data of **2** and **3** present some interesting questions with respect to the locations of the hydrogen substituents on the cyclopentadienyl ring. The existence of two different orientations of the hydrogen substituents in **2** is intriguing as well as its possible importance in making **1** crystallizable compared to $(C_5Me_4H)_2Sm(THF)_2$. Furthermore, the location of these hydrogen substituents in the back of the wedge would seem to allow for a more acute Cnt–Sm–Cnt angle. This is supported by the fact that the angle in complex **2** is 130° whereas the angle is 140° in $(C_5Me_5)_2Sm(DME)$. In complex **3**, which has the smallest Sm(II) Cnt–Sm–Cnt angle, 122.8°, only one hydrogen substituent is at the back of

the wedge of Sm(1) and the same is true for Sm(2) which has a coordination environment closest to complex **2**. Based on these results, there are clearly subtleties in the packing of tetramethylcyclopentadienyl complexes and these are likely to affect the solubility and crystallinity based on these results.

Given the results obtained with Sm(II) complexes with cyclopentadienyl ligands with one fewer methyl group than $(C_5Me_5)^{1-}$, it seems understandable that the chemistry of Sm(II) complexes of even less substituted cyclopentadienyl ligands is challenging in terms of solubility and crystallinity. Complexes such as $[(C_5H_5)_2Sm(THF)]_n$ and $[(C_5H_4Me)_2Sm(THF)]_n$ would be expected to oligomerize and could form a variety of bridging motifs.

4. Experimental Details

All manipulations and syntheses described below were conducted with the rigorous exclusion of air and water using standard Schlenk line and glovebox techniques under an argon atmosphere. Solvents were sparged with UHP argon and dried by passage through columns containing Q-5 and molecular sieves and stored over activated molecular sieves prior to use. Deuterated NMR solvents were dried over NaK alloy, degassed by three freeze-pump-thaw cycles, and vacuum transferred before use. ^{1}H NMR spectra were recorded on a Bruker AVANCE600 MHz spectrometer at 298 K unless otherwise stated and referenced internally to residual protio-solvent resonances. UV-visible spectra were collected in THF at 298 K using a Varian Cary 50 Scan UV-visible spectrometer in a 1 mm Schlenk cuvette fitted with a Teflon stopper unless otherwise stated. Infrared spectra were recorded as compressed solids on an Agilent Cary 630 ATR-FTIR. Elemental analyses were conducted on a Thermo Scientific FlashSmart CHNS/O Elemental Analyzer at UC Irvine Materials Research Institute's TEMPR facility in Irvine, California. $K(C_5Me_4H)$ [44] and $SmI_2(THF)_2$ [57] were synthesized according to literature procedures.

4.1. Synthesis of **1** *from* $SmI_2(THF)_2$ *and* $K(C_5Me_4H)$ *in THF*

In a glovebox containing coordinating solvents, solid $K(C_5Me_4H)$ (486 mg, 3.04 mmol) was added to a stirred dark blue solution of $SmI_2(THF)_2$ (827 mg, 1.51 mmol) in THF (5 mL) at room temperature. The mixture immediately turned dark purple with concomitant formation of white, insoluble precipitate. The mixture was stirred at room temperature overnight. After the white solids, presumably KI, were removed via centrifugation and filtration, solvent was removed under reduced pressure to yield purple solids. The purple solids were then washed with toluene (4 × 20 mL) until the washings were colorless and the toluene extracts and remaining purple solids (237 mg, 0.603 mmol, 40% assuming a $[(C_5Me_4H)_2Sm]_n$ product based on $SmI_2(THF)_2$) were separated. IR: 2939 w, 2870 m, 2847 s, 2722 w, 1435 m, 1386 m, 1315 w, 1025 w, 742 vs. UV-vis (THF, room temperature) λ_{max}, nm (ε, M^{-1} cm^{-1}): 395 (692), 549 (424). Anal. Calcd for **1**, presumed to be $[C_{18}H_{26}Sm]_n$: C, 55.04; H, 6.67. Found: C, 46.84; H, 5.897. C, 44.30; H, 5.582. C, 46.79; H, 5.876. Low C and H values were found across multiple runs and suggest incomplete combustion [45–49]. The C to H ratios in the analytical data give formulas of $C_{18}H_{27}$, $C_{18}H_{27}$, and $C_{18}H_{27}$, respectively, compared to the calculated value of $C_{18}H_{26}$.

4.2. Synthesis of $(C_5Me_4H)_2Sm^{II}(DME)$, **2**, *from* **1**

Compound **1** (237 mg) was dissolved in DME (10 mL), which immediately produced a dark green solution. Solvent was removed under reduced pressure to yield green solids (265 mg, 0.549 mmol, 36% based on $SmI_2(THF)_2$). Dark green crystals of **1**, suitable for study by X-ray diffraction, can be grown from a concentrated solution of **1** in DME stored at −35 °C. ^{1}H NMR (THF-d_8, 600 MHz): δ 15.28 (br s, 2H, $C_5Me_4\mathit{H}$), 9.21 (br s, 12H, $C_5\mathit{Me}_4H$), 3.38 (s, 4H, $CH_3OCH_2CH_2OCH_3$), 3.28 (s, 6H, $CH_3OCH_2CH_2OCH_3$), −0.32 (br s, 12H, $C_5\mathit{Me}_4H$) ppm. IR: 2859s, 2847s, 2715w, 2206w, 1440m, 1239w, 1189w, 1064 vs, 1015m, 853s, 743vs cm^{-1}. UV-vis (THF, room temperature) λ_{max}, nm (ε, M^{-1} cm^{-1}): 388 (995), 550 (488). Anal. Calcd for **2** $C_{22}H_{36}O_2Sm$: C, 54.72; H, 7.51. Found: C, 33.32; H, 7.51. C, 25.29; H,

3.72. C, 37.86; H, 5.33. Low C and H values were found across multiple runs and suggest incomplete combustion [45–49]. The C to H ratios in the analytical data give formulas of $C_{22}H_{37}$, $C_{22}H_{38.5}$, and $C_{22}H_{37}$, respectively, compared to the calculated value of $C_{22}H_{36}$.

4.3. Synthesis of $(C_5Me_4H)_2Sm^{II}(\mu\text{-}\eta^3\text{:}\eta^5\text{-}C_5Me_4H)Sm^{II}(C_5Me_4H)(THF)_2$, **3**

In a glovebox containing coordinating solvents, the dark purple-green toluene extract obtained from the procedure in 4.1 was concentrated under reduced pressure and stored at −35 °C. Over approximately 1 week, purple crystals of **3**, suitable for study by X-ray diffraction, were isolated (79 mg, 0.085 mmol, 11% based on $SmI_2(THF)_2$). IR: 2991 w, 2926 m, 2846 s, 2717 w, 1435 m, 1321 w, 1031 vs, 876 vs, 743 vs cm^{-1}. UV-vis (THF, room temperature) λ_{max}, nm (ε, M^{-1} cm^{-1}): 399 (1320), 552 (809). Anal. Calcd for **3** $C_{44}H_{68}O_2Sm_2$: C, 56.84; H, 7.37. Found: C, 55.28; H, 7.486. C, 51.53; H, 7.028. Low C and H values were found across multiple runs and suggest incomplete combustion [45–49]. The C to H ratios in the analytical data to give formulas of $C_{44}H_{71}$ and $C_{44}H_{71}$, respectively, compared to the calculated value of $C_{44}H_{68}$.

4.4. Direct Synthesis of $(C_5Me_4H)_2Sm(DME)$, **2**

In a glovebox containing coordinating solvents, solid $SmI_2(THF)_2$ (160 mg, 0.29 mmol) was added to a stirred suspension of $K(C_5Me_4H)$ (94 mg, 0.59 mmol) in 1,2-dimethoxyethane (5 mL) at room temperature, and the mixture gradually turned dark green over one minute. The mixture was allowed to stir at room temperature overnight. White, insoluble solids, presumably KI, were removed by centrifugation and filtration, and the resulting dark green solution was dried under reduced pressure to yield dark green solids. The solids were triturated with hexanes (2 mL) before being dried under reduced pressure to yield **1** as a dark green solid (132 mg, 0.273 mmol, 94%). Crystals of **1**, suitable for study by X-ray diffraction, were grown from a concentrated solution in DME stored at −35 °C overnight.

4.5. X-ray Data Collection, Structure Determination, and Refinement for $(C_5Me_4H)_2Sm(DME)$, **2**

A green crystal of approximate dimensions 0.114 × 0.209 × 0.481 mm was mounted in a cryoloop and transferred to a Bruker SMART APEX II diffractometer system. The APEX2 [58] program package was used to determine the unit-cell parameters and for data collection (30 sec/frame scan time). The raw frame data was processed using SAINT [59] and SADABS [60] to yield the reflection data file. Subsequent calculations were carried out using the SHELXTL [61] program package. The diffraction symmetry was *mmm* and the systematic absences were consistent with the orthorhombic space group *Pbca* that was later determined to be correct. The structure was solved by direct methods and refined on F^2 by full-matrix least-squares techniques. The analytical scattering factors [62] for neutral atoms were used throughout the analysis. Hydrogen atoms were included using a riding model. There were two molecules of the formula unit present. Least-squares analysis yielded wR2 = 0.0470 and Goof = 1.039 for 469 variables refined against 12,415 data (0.72 Å), R1 = 0.0195 for those 10,938 data with I > 2.0σ(I).

4.6. X-ray Data Collection, Structure Determination, and Refinement for $(C_5Me_4H)_2Sm(\mu\text{-}\eta^3\text{:}\eta^5\text{-}C_5Me_4H)Sm(C_5Me_4H)(THF)_2$, **3**

A purple crystal of approximate dimensions 0.170 × 0.191 × 0.306 mm was mounted in a cryoloop and transferred to a Bruker SMART APEX II diffractometer system. The APEX2 [58] program package was used to determine the unit-cell parameters and for data collection (20 s/frame scan time). The raw frame data was processed using SAINT [59] and SADABS [60] to yield the reflection data file. Subsequent calculations were carried out using the SHELXTL [61] program package. The diffraction symmetry was $2/m$ and the systematic absences were consistent with the monoclinic space group $P2_1/n$ that was later determined to be correct. The structure was solved by direct methods and refined on F^2 by full-matrix least-squares techniques. The analytical scattering factors [62] for neutral atoms were used throughout the analysis. Hydrogen atoms were included using a riding model.

Least-squares analysis yielded wR2 = 0.0536 and Goof = 1.021 for 449 variables refined against 12,542 data (0.70 Å), R1 = 0.0239 for those 10,610 data with I > 2.0σ(I).

4.7. X-ray Crystallographic Data

CCDC 2221542-2221543 contain the supplementary crystallographic data for this paper. These data can be obtained free of charge via www.ccdc.cam.ac.uk/data_request/cif (accessed on 1 December 2022), or by emailing data_request@ccdc.cam.ac.uk, or by contacting The Cambridge Crystallographic Data Centre, 12 Union Road, Cambridge CB2 1EZ, UK; Fax: +44-1223-336033. Crystal data, bond lengths and angles tables, and structure refinement information for complexes **2** and **3** can be found in the supporting information.

5. Conclusions

In conclusion, synthetic routes to two new crystallographically characterizable Sm(II) metallocenes have been discovered using $K(C_5Me_4H)$ and $SmI_2(THF)_2$ as starting materials. Although complex **2** adopts the typical monomeric Sm(II) bent metallocene structural motif, complex **3** is a rare example of an asymmetric bimetallic Sm(II)/Sm(II) complex bridged by a cyclopentadienyl ligand. The isolation of **3** provides supporting evidence for the possible oligomerization that may occur during the synthesis of Sm(II) metallocenes with less bulky and less solubilizing cyclopentadienyl ligands. This behavior can interfere with reactivity and can make the isolation and crystallization of reaction products more challenging. Reactivity studies are currently being pursued to investigate unusual differences in reactivity between $(C_5Me_5)_2Sm(THF)_2$ and complexes **2** and **3** as a result of switching from the pentamethylcyclopentadienyl ligand to the smaller and less substituted tetramethylcyclopentadienyl ligand.

Supplementary Materials: The following supporting information can be downloaded at: https://www.mdpi.com/article/10.3390/inorganics11010004/s1, Figures S1–S3: ^{1}H NMR spectra of compounds, $(C_5Me_4H)_2Sm(THF)_2$, **2**, and **3**, respectively; Figures S4–S6: Infrared spectra of compounds **1**, **2**, and **3**, respectively; Figures S7–S11: UV-visible spectra of **1** in THF, **2** in THF, **3** in THF, **3** in toluene, and $(C_5Me_5)_2Sm(THF)_2$ in THF, respectively; Tables S1 and S2: Crystal data, bond lengths, and bond angles of **2**; Tables S3 and S4: Crystal data, bond lengths, and bond angles of **3**.

Author Contributions: Conceptualization, J.Q.N. and W.J.E.; Methodology, J.Q.N. and W.J.E.; Formal analysis, J.Q.N. and J.W.Z.; Investigation, J.Q.N.; Writing—original draft, J.Q.N. and W.J.E.; Writing—review & editing, J.Q.N. and W.J.E.; Supervision, J.W.Z. and W.J.E.; Project administration, W.J.E.; Funding acquisition, W.J.E. All authors have read and agreed to the published version of the manuscript.

Funding: This research was funded by the U. S. National Science Foundation, grant number CHE-2154255 (to W.J.E.) and the APC was funded by the MDPI.

Data Availability Statement: Spectroscopic data and detailed crystallographic information can be found in the supplementary materials. Crystallographic data are available via the Cambridge Crystallographic Data Centre (CCDC): 2221542-2221543.

Acknowledgments: We thank the U.S. National Science Foundation for support of the experimental parts of this research under CHE-2154255 (to W.J.E) and the MDPI for funding the APC.

Conflicts of Interest: The authors declare no competing financial interest.

References

1. Evans, W.J.; Bloom, I.; Hunter, W.E.; Atwood, J.L. Synthesis and X-ray Crystal Structure of a Soluble Divalent Organosamarium Complex. *J. Am. Chem. Soc.* **1981**, *103*, 6507–6508. [CrossRef]
2. Evans, W.J.; Hughes, L.A.; Hanusa, T.P. Synthesis and Crystallographic Characterization of an Unsolvated, Monomeric Bis(pentamethylcyclopentadienyl) Organolanthanide Complex, $(C_5Me_5)_2Sm$. *J. Am. Chem. Soc.* **1984**, *106*, 4270–4272. [CrossRef]
3. Evans, W.J.; Grate, J.W.; Hughes, L.A.; Zhang, H.; Atwood, J.L. Reductive homologation of carbon monoxide to a ketenecarboxylate by a low-valent organolanthanide complex: Synthesis and x-ray crystal structure of $[(C_5Me_5)_4Sm_2(O_2CCCO)(THF)]_2$. *J. Am. Chem. Soc.* **1984**, *107*, 3728–3730. [CrossRef]

4. Evans, W.J.; Hughes, L.A.; Drummond, D.K.; Zhang, H.; Atwood, J.L. Facile Stereospecific Synthesis of a Dihydroxyindenoindene Unit from an Alkyne and Carbon Monoxide via Samarium-Mediated Carbon Monoxide and CH Activation. *J. Am. Chem. Soc.* **1986**, *108*, 1722–1723. [CrossRef]
5. Evans, W.J.; Drummond, D.K. Insertion of two carbon monoxide moieties into an alkene double bond to form a RCH:C(O)C(O):CHR^{2-} unit via organosamarium activation. *J. Am. Chem. Soc.* **1988**, *110*, 2772–2774. [CrossRef]
6. Evans, W.J.; Ulibarri, T.A.; Ziller, J.W. Reactivity of $(C_5Me_5)_2Sm$ with Aryl-Substituted Alkenes: Synthesis and Structure of a Bimetallic Styrene Complex That Contains an η^2-Arene Lanthanide Interaction. *J. Am. Chem. Soc.* **1990**, *112*, 219–223. [CrossRef]
7. Evans, W.J.; Keyer, R.A.; Rabe, G.W.; Drummond, D.K.; Ziller, J.W. The Reactivity of $(C_5Me_5)_2Sm(THF)_2$ with Bis(2-Pyridyl)Ethene Including the Synthesis of $[(C_5Me_5)_2Sm]_2(\mu\text{-}\eta^2\text{:}\eta^2\text{-PyCHCHpy})]$ from $[(C_5Me_5)_2Sm]_2[\mu\text{-}\eta^3\text{:}\eta^3\text{-1,2,3,4-(Py)}_4C_4H_4]$ by Reductive C-C Bond Cleavage. *Organometallics* **1993**, *12*, 4664–4667. [CrossRef]
8. Evans, W.J.; Ulibarri, T.A.; Ziller, J.W. Isolation and X-Ray Crystal Structure of the First Dinitrogen Complex of an *f*-Element Metal, $[(C_5Me_5)_2Sm]_2N_2$. *J. Am. Chem. Soc.* **1988**, *110*, 6877–6879. [CrossRef]
9. Swamy, S.J.; Loebel, J.; Pickardt, J.; Schumann, H. Organometallic compounds of the lanthanides XLVI. Synthesis and crystallographic characterization of $(C_5Me_5)_2Sm(DME)$. *J. Organomet. Chem.* **1988**, *353*, 27–34. [CrossRef]
10. Gagné, M.R.; Nolan, S.P.; Marks, T.J. Organolanthanide-Centered Hydroamination/Cyclization of Aminoolefins. Expedient Oxidative Access to Catalytic Cycles. *Organometallics* **1990**, *9*, 1716–1718. [CrossRef]
11. Recknagel, A.; Noltemeyer, M.; Edelmann, F.T. Organolanthanid(II)chemie: Reaktionen von $Cp^*_2Sm(THF)_2$ mit 1,4-Diazadinen und Cyclooctatetraen. *J. Organomet. Chem.* **1991**, *410*, 53–61. [CrossRef]
12. Wang, K.-G.; Stevens, E.D.; Nolan, S.P. Synthesis and structural characterization of a tetranuclear organolanthanide hydrazido complex. *Organometallics* **1992**, *11*, 1011–1013. [CrossRef]
13. Rieckhoff, M.; Noltemeyer, M.; Edelmann, F.T.; Haiduc, I.; Silaghi-Dumitrescu, I. Ein alter Ligand in neuer Umgebung: Dreifach verbrückendes O, Ó-Dimethyldithiophosphat im Organosamarium-Komplex $[(C_5Me_5)Sm\{S_2P(OMe)_2\}_2]_2$. *J. Organomet. Chem.* **1994**, *469*, C19–C21. [CrossRef]
14. Makioka, Y.; Koyama, K.; Nishiyama, T.; Takaki, K.; Taniguchi, Y.; Fujiwara, Y. Generation of Allenic Samarium Complexes from Propargylic Ethers and $(C_5Me_5)_2Sm(thf)_2$, and Their Electrophilic Trapping. *Tetrahedron Lett.* **1995**, *36*, 6283–6286. [CrossRef]
15. Takeno, M.; Kikuchi, S.; Morita, K.; Nishiyama, Y.; Ishii, Y. A New Coupling Reaction of Vinyl Esters with Aldehydes Catalyzed by Organosamarium Compounds. *J. Org. Chem.* **1995**, *60*, 4974–4975. [CrossRef]
16. Takaki, K.; Maruo, M.; Kamata, T.; Makioka, Y.; Fujiwara, Y. Selective C-O Bond Cleavage of Vinyl Ethers with $Cp^*_2Sm(thf)_n$ Leading to Vinylsamarium or Enolate Complexes. *J. Org. Chem.* **1996**, *61*, 8332–8334. [CrossRef]
17. Tashiro, D.; Kawasaki, Y.; Sakaguchi, S.; Ishii, Y. An Efficient Acylation of Tertiary Alcohols with Isoproprenyl Acetate Mediated by an Oxime Ester and $Cp^*_2Sm(thf)_2$. *J. Org. Chem.* **1997**, *62*, 8141–8144. [CrossRef]
18. Nomura, R.; Shibasaki, Y.; Endo, T. Transformation of the cationic growing center of poly(tetrahydrofuran) into an anionic one by bis(pentamethylcyclopentadienyl)samarium. *J. Polym. Sci. Part A Polym. Chem.* **1998**, *36*, 2209–2214. [CrossRef]
19. Kefalidis, C.E.; Essafi, S.; Perrin, L.; Maron, L. Qualitative Estimation of the Single-Electron Transfer Step Energetics Mediated by Samarium(II) Complexes: A "SOMO–LUMO Gap" Approach. *Inorg. Chem.* **2009**, *53*, 3427–3433. [CrossRef]
20. Konchenko, S.N.; Pushkarevsky, N.A.; Gamer, M.T.; Köppe, R.; Schnöckel, H.; Roesky, P.W. $[\{(\eta^5\text{-}C_5Me_5)_2Sm\}_4P_8]$: A Molecular Polyphosphide of the Rare-Earth Elements. *J. Am. Chem. Soc.* **2009**, *131*, 5740–5741. [CrossRef]
21. Li, T.; Gamer, M.T.; Scheer, M.; Konchenko, S.N.; Roesky, P.W. P–P bond formation *via* reductive dimerization of $[Cp^*Fe(n^5\text{-}P_5)]$ by divalent samarocenes. *Chem. Commun.* **2013**, *49*, 2183–2185. [CrossRef] [PubMed]
22. Klementyeva, S.V.; Gritsan, N.P.; Khusniyarov, M.M.; Witt, A.; Dmitriev, A.A.; Suturina, E.A.; Hill, N.D.D.; Roemmele, T.L.; Gamer, M.T.; Boeré, R.T.; et al. The First Lanthanide Complexes with a Redox-Active Sulfur Diimide Ligand: Synthesis and Characterization of $[LnCp^*_2(RN{=})_2S]$, Ln = Sm, Eu, Yb; R = $SiMe_3$. *Chem. Eur. J.* **2017**, *23*, 1278–1290. [CrossRef] [PubMed]
23. Pushkarevsky, N.A.; Ilyin, I.Y.; Petroc, P.A.; Samsonenko, D.G.; Ryzhikov, M.R.; Roesky, P.W.; Konchenko, S.N. Different Reductive Reactivities of $SmCp^x_2(THF)_n$ (Cp^x= C_5Me_5 and $C_5H_3{}^tBu_2$) Samarocenes toward P_2Ph_4: THF Ring-Opening and Ligand-Exchange Pathways. *Organometallics* **2017**, *36*, 1287–1295. [CrossRef]
24. Schoo, C.; Bestgen, S.; Egeberg, A.; Klementyeva, S.; Feldmann, C.; Konchenko, S.N.; Roesky, P.W. Samarium Polystibides Derived from Highly Activated Nanoscale Antimony. *Angew. Chem. Int. Ed.* **2018**, *57*, 5912–5916. [CrossRef] [PubMed]
25. Schoo, C.; Bestgen, S.; Egeberg, A.; Siebert, J.; Konchenko, S.N.; Feldmann, C.; Roesky, P.W. Samarium Polyarsenides Derived from Nanoscale Arsenic. *Angew. Chem. Int. Ed.* **2019**, *58*, 4386–4389. [CrossRef] [PubMed]
26. Watt, G.W.; Gillow, E.W. Samarium(II) dicyclopentadienide 1-tetrahydrofuranate. *J. Am. Chem. Soc.* **1969**, *91*, 775–776. [CrossRef]
27. Evans, W.J. Organometallic Lanthanide Chemistry. *Adv. Organomet. Chem.* **1985**, *24*, 131–177. [CrossRef]
28. Evans, W.J. The Organometallic Chemistry of the Lanthanide Elements in Low Oxidation States. *Polyhedron* **1987**, *6*, 803–835. [CrossRef]
29. Sitzmann, H.; Dezember, T.; Schmitt, O.; Weber, F.; Wolmershäuser, G. Reactions of Free Cyclopentadienyl Radicals. 3 Metallocenes of Samarium, Europium, and Ytterbium with the Especially Bulky Cyclopentadienyl Ligands $C_5H(CHMe_2)_4$, $C_5H_2(CMe_3)_3$, and $C_5(CHMe_2)_5$. *Z. Anorg. Allg. Chem.* **2000**, *626*, 2241–2244. [CrossRef]
30. Kelly, R.P.; Bell, T.D.M.; Cox, R.P.; Daniels, D.P.; Deacon, G.B.; Jaroschik, F.; Junk, P.C.; Le Goff, X.F.; Lemercier, G.; Martinez, A.; et al. Divalent Tetra- and Penta-phenylcyclopentadienyl Europium and Samarium Sandwich and Half-Sandwich Complexes: Synthesis, Characterization, and Remarkable Luminescence Properties. *Organometallics* **2015**, *34*, 5624–5636. [CrossRef]

31. Evans, W.J.; Gummersheimer, T.S.; Boyle, T.J.; Ziller, J.W. Synthesis and Structure of New Soluble Organosamarium(II) Reagents: $(indenyl)_2Sm(THF)$ and $(fluorenyl)_2Sm(THF)_2$. *Organometallics* **1994**, *13*, 1281–1284. [CrossRef]
32. Evans, W.J.; Forrestal, K.J.; Ziller, J.W. Isopropyltetramethylcyclopentadienyl samarium chemistry: Structural studies of divalent $(C_5Me_4{}^iPr)_2Sm(THF)$ and mixed valent $[(C_5Me_4{}^iPr)_2Sm]_2(\mu\text{-}Cl)$. *Polyhedron* **1998**, *17*, 4015–4021. [CrossRef]
33. Evans, W.J.; Kociok-Köhn, G.; Foster, S.E.; Ziller, J.W.; Doedens, R.J. Synthesis and structure of mono-THF solvates of bis(cyclopentadienyl)samarium(II) complexes: $(C_5Me_5)_2Sm(THF)$ and $[C_5H_2(SiMe_3)_3][C_5H_3(SiMe_3)_2]Sm(THF)$. *J. Organomet. Chem.* **1993**, *444*, 61–66. [CrossRef]
34. Yatabe, T.; Karasawa, M.; Isobe, K.; Ogo, S.; Nakai, H. A napthyl-substituted pentamethylcyclopentadienyl ligand and its Sm(II) bent-metallocene complexes with solvent-induced structure change. *Dalton Trans.* **2012**, *41*, 354–356. [CrossRef]
35. Ruspic, C.; Moss, J.R.; Schürmann, M.; Harder, S. Remarkable Stability of Metallocenes with Superbulky Ligands: Spontaneous Reduction of Sm^{III} to Sm^{II}. *Angew. Chem. Int. Ed.* **2008**, *47*, 2121–2126. [CrossRef] [PubMed]
36. van Velzen, N.J.C.; Harder, S. Deca-Arylsamarocene: An Unusually Inert Sm(II) Sandwich Complex. *Organometallics* **2018**, *37*, 2263–2271. [CrossRef]
37. Evans, W.J.; Perotti, J.M.; Brady, J.C.; Ziller, J.W. Tethered Olefin Studies of Alkene versus Tetraphenylborate Coordination and Lanthanide Olefin Interactions in Metallocenes. *J. Am. Chem. Soc.* **2003**, *125*, 5204–5212. [CrossRef]
38. Visseaux, M.; Barbier-Baudry, D.; Blacque, O.; Hafid, A.; Richard, P.; Weber, F. New base-free metallocenes of samarium and neodymium, an approach to stereoelectronic control in organolanthanide chemistry. *New J. Chem.* **2000**, *24*, 939–942. [CrossRef]
39. Shephard, A.C.G.; Daniels, D.P.; Deacon, G.B.; Guo, Z.; Jaroschik, F. Junk, P.C. Selective carbon-phosphorus bond cleavage: Expanding the toolbox for accessing bulky divalent lanthanoid sandwich complexes. *Chem. Commun.* **2022**, *58*, 4344–4347. [CrossRef]
40. Selikhov, A.N.; Mahrova, T.V.; Cherkasov, A.V.; Fukin, G.K.; Larionova, J.; Long, J.; Trifonov, A.A. Base-Free Lanthanoidocenes(II) Coordinated by Bulky Pentabenzylcyclopentadienyl Ligands. *Organometallics* **2015**, *34*, 1991–1999. [CrossRef]
41. Schumann, H.; Meese-Marktscheffel, J.A.; Esser, L. Synthesis, Structure, and Reactivity of Organometallic π-Complexes of the Rare Earths in the Oxidation State Ln^{3+} with Aromatic Ligands. *Chem. Rev.* **1995**, *95*, 865–986. [CrossRef]
42. Schumann, H.; Glanz, M.; Hemling, H.; Hahn, F.E. Organometallic Compounds of the Lanthanides. 93. Tetramethylcyclopentadienyl Complexes of Selected 4*f*-Elements. *Z. Anorg. Allg. Chem.* **1995**, *621*, 341–345. [CrossRef]
43. Schultz, M.; Burns, C.J.; Schwartz, D.J.; Andersen, R.A. Solid-State Structures of Base-Free Ytterbocenes and Inclusion Compounds of Bis(pentamethylcyclopentadienyl)ytterbium with Neutral Carboranes and Toluene: The Role of Intermolecular Contacts. *Organometallics* **2000**, *19*, 781–789. [CrossRef]
44. Goodwin, C.A.P.; Su, J.; Stevens, L.M.; White, F.D.; Anderson, N.H.; Auxier, J.D., II; Albrecht-Schönzart, T.E.; Batista, E.R.; Briscoe, S.F.; Cross, J.N.; et al. Isolation and Characterization of a Californium Metallocene. *Nature* **2021**, *59*, 421–424. [CrossRef]
45. Hitchcock, P.B.; Lappert, M.F.; Maron, L.; Protchenko, A.V. Lanthanum Does Form Stable Molecular Compounds in the +2 Oxidation State. *Angew. Chem. Int. Ed.* **2008**, *120*, 1488–1491. [CrossRef]
46. Goodwin, C.A.P.; Joslin, K.C.; Lockyer, S.J.; Formanuik, A.; Morris, G.A.; Ortu, F.; Vitorica-Yrezabal, I.J.; Mills, D.P. Homoleptic Trigonal Planar Lanthanide Complexes stabilized by Silylamide Ligands. *Organometallics* **2015**, *34*, 2314–2325. [CrossRef]
47. Chilton, N.F.; Goodwin, C.A.P.; Mills, D.P.; Winpenny, R.E.P. The first near-linear bis(amide) *f*-block complex: A blueprint for a high temperature single molecule magnet. *Chem. Commun.* **2015**, *51*, 101–103. [CrossRef]
48. Gabbaï, F.P.; Chirik, P.J.; Fogg, D.E.; Meyer, K.; Mindiola, D.J.; Schafer, L.L.; You, S.L. An Editorial about Elemental Analysis. *Organometallics* **2016**, *35*, 3255–3256. [CrossRef]
49. Ortu, F.; Packer, D.; Liu, J.; Burton, M.; Formanuik, A.; Mills, D.P. Synthesis and structural characterization of lanthanum and cerium substituted cyclopentadienyl borohydride complexes. *J. Organomet. Chem.* **2018**, *857*, 45–51. [CrossRef]
50. Evans, W.J.; Ulibarri, T.A. Reactivity of $(C_5Me_5)_2Sm$ with cyclopentadiene and cyclopentadienide: Isolation of the mixed-valence complex $(C_5Me_5)_2Sm^{III}(\mu\text{-}C_5H_5)Sm^{II}(C_5Me_5)_2$. *J. Am. Chem. Soc.* **1987**, *109*, 4292–4297. [CrossRef]
51. Evans, W.J.; Ulibarri, T.A.; Ziller, J.W. Reactivity of $(C_5Me_5)_2Sm$ and Related Species with Alkenes: Synthesis and Structural Characterization of a Series of Organosamarium Allyl Complexes. *J. Am. Chem. Soc.* **1990**, *112*, 2314–2324. [CrossRef]
52. Evans, W.J.; Kozimor, S.A.; Ziller, J.W. Methyl Displacements from Cyclopentadienyl Ring Planes in Sterically Crowded $(C_5Me_5)_3M$ Complexes. *Inorg. Chem.* **2005**, *44*, 7960–7969. [CrossRef] [PubMed]
53. Cotton, F.A.; Marks, T.J. An Infrared Study of the Structures of Cyclopentadienyl Compounds of Copper(I) and Mercury(II). *J. Am. Chem. Soc.* **1969**, *91*, 7281–7285. [CrossRef]
54. Clark, R.J.H.; Lewis, J.; Machin, D.J.; Nyholm, R.S. 59. Complexes of titanium trichloride. *J. Chem. Soc.* **1963**, 379–387. [CrossRef]
55. Lewis, J.; Miller, J.R.; Richards, R.L.; Thompson, A. 1098. The infrared spectra of some addition compounds of aluminum and gallium trihalides. *J. Chem. Soc.* **1965**, 5850–5860. [CrossRef]
56. Clark, D.L.; Frankcom, T.M.; Miller, M.M.; Watkin, J.G. Facile solution routes to hydrocarbon-soluble Lewis base adducts of thorium tetrahalides. Synthesis, characterization, and X-ray structure of $ThBr_4(THF)_4$. *Inorg. Chem.* **1992**, *31*, 1628–1633. [CrossRef]
57. Girard, P.; Namy, J.L.; Kagan, H.B. Divalent lanthanide derivatives in organic synthesis, 1. Mild preparation of samarium iodide and ytterbium iodide and their use as reducing or coupling agents. *J. Am. Chem. Soc.* **1980**, *102*, 2693–2698. [CrossRef]
58. *APEX2*, Version 2014.11-0; Bruker AXS, Inc.: Madison, WI, USA, 2014.
59. *SAINT*, Version 8.34a; Bruker AXS, Inc.: Madison, WI, USA, 2013.

60. Sheldrick, G.M. *SADABS*, Version 2014/5; Bruker AXS, Inc.: Madison, WI, USA, 2014.
61. Sheldrick, G.M. *SHELXTL*, Version 2014/7; Bruker AXS, Inc.: Madison, WI, USA, 2014.
62. *International Tables for Crystallography 1992, Volume C*, Kluwer Academic Publishers: Dordrecht, The Netherlands, 2004.